Chemical Engineering Journal 268 (2015) 280–289

Contents lists available at ScienceDirect

Chemical Engineering Journal

journal homepage: www.elsevier.com/locate/cej

Iron–alumina synergy in the heterogeneous Fenton-type peroxidation of phenol solutions

C. di Luca *, F. Ivorra, P. Massa, R. Fenoglio

INTEMA/Facultad de Ingeniería, Universidad Nacional de Mar del Plata, Juan B. Justo 4302, 7600 Mar del Plata, Argentina

HIGHLIGHTS

- Mesoporous alumina-supported Fe catalysts were developed (0.5–4% Fe).
- The systems were applied in the phenol catalytic peroxidation reaction at 70 °C.
- A synergistic effect between Fe–Al might improve the catalytic performance.
- Catalytic activity was enhanced due to high dispersion over the alumina support.
- High mineralization levels (up to 80%) and efficient H_2O_2 consumption were reached.

GRAPHICAL ABSTRACT

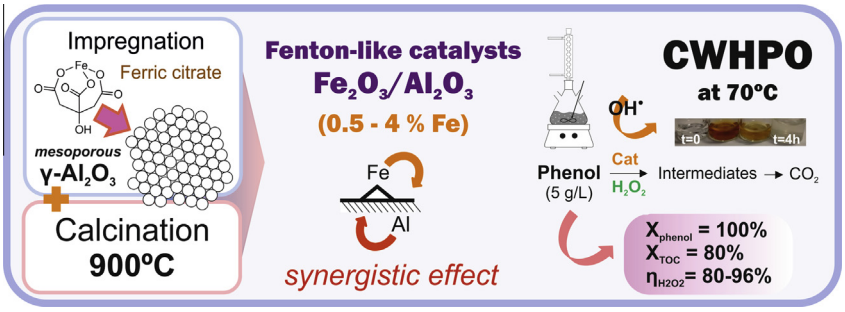

ARTICLE INFO

Article history:
Received 28 October 2014
Received in revised form 17 January 2015
Accepted 19 January 2015
Available online 28 January 2015

Keywords:
$Fe–Al_2O_3$
Mesoporous alumina
CWHPO
Phenol
Heterogeneous Fenton-like systems

ABSTRACT

Highly dispersed Fe_2O_3/Al_2O_3 catalysts (0.5–4 wt% Fe) were prepared by incipient wetness impregnation of iron citrate over a mesoporous alumina host. Their structural and textural properties were determined by N_2 adsorption–desorption at −196 °C, XRD, TEM, SEM–EDAX, Raman and XPS. The structure of the catalytic materials resulted similar to the γ-Al_2O_3 support, exhibiting high dispersion levels of the iron oxide active phase with a narrow pore size distribution in the range of 2–7 nm and high surface areas. The capability of these systems as efficient and active Fenton-like catalysts, were further tested for the catalytic oxidation of concentrated phenol solutions (5 g/L) with H_2O_2 at 70 °C in a batch reactor. The effects of iron concentration, catalyst concentration and the nature of the support were evaluated, under adjusted sub-stoichiometric oxidant concentration. Besides the positive impact of increasing the iron loading, a synergistic effect between Fe and Al species would be possibly responsible of the improvements observed using higher iron dispersions and/or support concentrations. The catalytic performance of these alumina-based catalysts resulted very promissory as they yielded: total phenol abatement, high mineralization levels (up to a maximum of 80%) and high oxidant consumption efficiencies (between 80% and 96%).

1. Introduction

The development of catalytic materials for water remediation is a topic under growing research. The current demands of more efficient and economic treatment solutions necessarily involve environmentally friendly procedures. In this context, the application of advanced oxidation technologies (AOTs) have emerged as very promising alternatives due to their excellent capability for the mineralization of toxic or highly refractory organic compounds. AOTs include a series of methods that generate strongly oxidative radicals to degrade pollutant molecules. The use of the classic Fenton reaction ($Fe(II)/H_2O_2$) can be classified as a non-photochemical

* Corresponding author. Tel.: +54 0223 4816600/242; fax: +54 0223 4810046.
E-mail addresses: cardiluca@gmail.com (C. di Luca), fivorra@fi.mdp.edu.ar (F. Ivorra), pamassa@fi.mdp.edu.ar (P. Massa), rofeno@mdp.edu.ar (R. Fenoglio).

http://dx.doi.org/10.1016/j.cej.2015.01.074
1385-8947/

AOT. More recent approaches have aimed to overcome some of the major drawbacks of the Fenton system (e.g., separation/recuperation of the homogeneous catalyst, ineffective consumption of the H_2O_2, acid-range pH adjustment requirements) by immobilizing transition cations (mostly Fe but not exclusively) on solid supports in the so-called heterogeneous Fenton processes. A variety of materials have been investigated [1–4]; however, up to the present only a relatively limited number of these studies have explored the advantages of using alumina-based catalysts [5–10]. Table 1 reviews main results on the abatement of organic pollutants by means of Catalytic Wet Hydrogen Peroxide Oxidation (CWHPO) under mild operating conditions, in presence of Fe–Al solid catalysts; for comparative purposes Cu–alumina and Fe–silica materials were also included. As can be observed, the reaction tests were performed under different operating conditions, such as catalyst load, initial Total Organic Carbon (TOC), H_2O_2 concentration, temperature, reaction time and pH, as well as diverse catalyst preparation methodologies.

Al_2O_3 is a widely used adsorbent and a typical catalyst support. Some forms of transitional alumina (e.g., γ-Al_2O_3) are useful as catalysts or co-catalysts due to a favourable combination of textural properties, acid–base characteristics and on the degree of hydration and hydroxylation of the surface [16]. The extent of these features is strongly dependant on the preparation and pretreatment conditions [17]. During the catalyst preparation steps, the adsorption phenomena take a significant part since most of the precursors are incorporated via impregnation. After the impregnation process, alumina has been reported to play an essential part in the formation of active sites. This support is also able to adsorb reactants in the course of reactions and this may be beneficial for the catalytic activity and selectivity [18].

In the case of mesoporous aluminas, they are characterized by narrow mesopore size distributions with average pore diameters in the range of 3–7 nm. Due to their high surface area they provide higher density of active sites. As well with the presence of Bronsted and Lewis acid sites, these materials present a relatively high density of basic sites which promote strong interactions between metal oxides and the alumina support, thereby improving the catalytic performance [19].

Our group have amply investigated gamma alumina-supported catalytic materials for the abatement of water pollutants. In a previous work, we studied the performance of Fe_2O_3/γ-Al_2O_3 (2 wt% Fe) catalysts in the peroxidation of model phenol solutions (0.5–5 g/L) at mild operating conditions [9]. The systems resulted active but they exhibited relatively controlled H_2O_2 consumption rates. Therefore, we adjusted the H_2O_2 initial concentrations to obtain more efficient oxidant consumptions. We also registered that catalysts stability could be enhanced by using a simple preparation methodology (wet impregnation followed by 900 °C calcination) that promoted good active phase dispersion levels and a marked decrease in the iron leaching, with no significant reduction of the final mineralization percentages. From these results, the catalysts preparation procedure and the reaction variables were adjusted in order to improve the catalytic performance at demanding operating conditions.

For the present study, the synthetic effluents were prepared using a high organic carbon content of 3.5 g/L, chosing phenol as model recalcitrant contaminant [20]. While several works dealt with the abatement of low concentration phenolic solutions ($[TOC]_0$ = 76.6 mg/L), Fenton-type reaction is more effective for medium–high organic contents (typically higher than 0.5 g TOC/L) [21]. Throughout this work a relatively concentrated phenol initial charge (5 g/L) was selected; this concentration represents an upper limit within the range of concentrations commonly found in phenolic industrial effluents [20]. However, better catalytic performances (in terms of activity and stability) can be expected by using lower organic concentrations [9].

Along with some major reaction variables such as temperature or pH, the oxidant dose and the concentration of iron species should be also considered as key parameters in the Fenton processes [22]. In particular, the yield of hydrogen peroxide use is a very critical parameter for CWHPO reactions, as the solid catalysts may also catalyze H_2O_2 side decomposition to H_2O and O_2. This parameter depends considerably on the reaction conditions, principally on the modality of the oxidant addition and on the ratio between catalyst load and volume of solution [23].

In this study, the performance of mesoporous Fe_2O_3/γ-Al_2O_3 materials was tested in the CWHPO of phenolic solutions. We aimed to investigate the impact of the total iron concentration, the catalyst concentration and the influence of the alumina support in the performance of heterogeneous Fenton-like systems, followed in terms of phenol and TOC removal and oxidant consumption efficiency. The purpose was to explore the potential advantages of economical catalytic materials (i.e., base-metal oxides) enhanced through simple procedures to be used for water pollutant abatement applications.

2. Experimental

2.1. Catalysts preparation and characterization

The Fe_2O_3/γ-Al_2O_3 catalysts were prepared by incipient wetness impregnation of commercial γ-Al_2O_3 (ALFA AESAR, spheres, 1.1 mm) using an aqueous solution of iron citrate (Cicarelli, p.a.) as precursor. After impregnation, the sample was left for 12 h at room temperature and calcined at 900 °C, under air current (10 L/min) for 4 h. The total iron content of the samples ranged between 0.5 and 4 wt% Fe. Table 2 summarizes the iron contents of the four different samples, designed as 0.5FeAl, 1FeAl, 2FeAl and 4FeAl.

The iron determination was performed by a standard colorimetric test (FerroVer® Iron Reagent, HACH), with a previous nitric acid extraction of the solid samples. Final leaching levels were estimated by comparing the initial and final iron contents of the used catalysts.

The support and the catalysts were also characterized using the following techniques:

- *Nitrogen Physisorption.* The nitrogen adsorption and desorption isotherms at −196 °C were measured using a Quadrasorb SI equipment. Specific surface areas were calculated from the adsorption branches by the BET method, while pore size distribution were deduced from the desorption branches. Before analysis, each sample was degassed overnight at 120 °C under vacuum conditions.
- *X-ray diffraction (XRD).* Powder X-ray diffraction patterns of the catalysts were obtained with a PANalytical X'Pert Pro diffractometer by using nickel-filtered Cu Kα radiation. The patterns were recorded over $10° < 2\theta < 70°$ range and compared to the JCPDS files to confirm phase identities. The main peaks corresponding to the gamma alumina phase are: $2\theta = 66.7°$ (100); 46.1° (80); 37.4° (60); 39.7° (30).
- *Transmission Electron Microscopy (TEM).* The microstructure of the materials was studied using a JEOL TEM-1011 instrument operating at an accelerating voltage of 100 kV. Samples were prepared by dispersing the powdered catalysts in ethanol and then dropping the suspension onto a standard formvar-coated copper grid.

Table 1
CWHPO of organic pollutants by Fe–Al heterogeneous catalysts under mild reaction conditions (for comparative purposes Cu–Al and Fe–Si systems were also included).

Catalyst	Preparation method	Pollutant (P)	Results	Leaching	Operating conditions[a]	Ref.
7.7 wt% Fe/Al_2O_3 powder	Impregnation Fe(III) nitrate on γ-Al_2O_3 (Rhone Poulanc, 145–205 m^2/g) ox. 450 °C	Phenol $[TOC]_0$ = 72 mg/L	X_{TOC} = 50% X_P = 100% $X_{H_2O_2}$ = 47%	8% (6.5 mg/L)	T = *RT*, P atm [cat] = 1 g/L R = 1.07 $t_{reaction}$ = 120 min pH not controlled	[5]
2 wt% Fe/Al_2O_3 powder	Precipitation Fe(III) nitrate on α-Al_2O_3 (3 m^2/g) ox. 500 °C	Phenol $[TOC]_0$ = 720 mg/L	X_{TOC} = 26% X_P = 100% $X_{H_2O_2}$ = 100%	21% (21 mg/L)	T = 90 °C, P atm [cat] = 5 g/L R = 0.71 $t_{reaction}$ = 180 min pH not controlled	[11]
4 wt% Fe/Al_2O_3 powder	Commercial Fe/γ-Al_2O_3 (IC-12-74)	Phenol $[TOC]_0$ = 720 mg/L	X_{TOC} = 56% X_P = 98% $X_{H_2O_2}$ = 100%	5% (10 mg/L)	T = 90 °C, P atm [cat] = 5 g/L R = 0.71 $t_{reaction}$ = 180 min pH not controlled	[11]
2 wt% Fe/Al_2O_3 pellet (2–3 mm)	Impregnation Fe(III) nitrate on γ-Al_2O_3 (201 m^2/g) ox. 350 °C	Acid Orange 52 $[TOC]_0$ = 260 mg/L	X_{TOC} = 75% 81% discolouration $X_{H_2O_2}$ = 47%	Negligible 0.04 mg/L	T = *RT*, P atm [cat] = 30 g/L $[H_2O_2]_0$ = 9.7 mM $t_{reaction}$ = 180 min pH not controlled	[6]
3.9 wt% Fe/Al_2O_3 powder	Impregnation Fe(III) nitrate on γ-Al_2O_3 (Merck, 142 m^2/g) ox. 300 °C	Phenol $[TOC]_0$ = 76.6 mg/L	X_{TOC} = 78% X_P = 100% $X_{H_2O_2}$ = 81%	~2% (0.9 mg/L)	T = 50 °C, P atm [cat] = 1.25 g/L R = 1 $t_{reaction}$ = 480 min pH_0 = 3	[7]
		Phenol $[TOC]_0$ = 1150 mg/L	X_{TOC} = 45% X_P = 99% $X_{H_2O_2}$ = 54%	15% (7.4 mg/L)		
3.8 wt% Fe/Al_2O_3 powder	Impregnation Fe(III) nitrate on γ-Al_2O_3 (Merck, 141 m^2/g) ox. 300 °C red. 350 °C	4-Chlorophenol $[TOC]_0$ = 56 mg/L	X_{TOC} ≈ 75% X_P = 100% $X_{H_2O_2}$ = 80%	6% (⩽3 mg/L)	T = 50 °C, P atm [cat] = 1 g/L R = 1 $t_{reaction}$ = 240 min pH_0 = 3	[10]
0.4 wt% Fe/Al_2O_3 pellet (2.5 mm)	Adsorption of Prussian Blue NPs on γ-Al_2O_3 (SASOL, 224 m^2/g) *not calcined*	Orange G $[TOC]_0$ = 38 mg/L	X_{TOC} = 60% 100% discolouration $X_{H_2O_2}$ = 100%	3% (0.7 mg/L)	T = 70 °C, P atm [cat] = 6.5 g/L R = 1 $t_{reaction}$ = 300 min pH_0 = 3	[12]
5 wt% Fe/Al_2O_3 powder	Impregnation (Fe(III), NH_4)-citrate on mesoporous Al_2O_3 ox. 450 °C	Phenol $[TOC]_0$ = 36 mg/L	X_{TOC} = 67% X_P = 100% $X_{H_2O_2}$ = *not reported*	1% (0.43 mg/L)	T = *RT*, P atm [cat] = 1 g/L R = 1.14 $t_{reaction}$ = 240 min pH_0 = 3.7	[13]
Al–Fe pillared clay (3 wt% Fe) powder	Pillaring commercial bentonite by Al–Fe species 180 m^2/g ox. 500 °C	Phenol $[TOC]_0$ = 36 mg/L	X_{TOC} = 65% X_P = 100% $X_{H_2O_2}$ = *not reported*	Negligible 0.2 mg/L	T = *RT*, P atm [cat] = 5 g/L R = 1.14 $t_{reaction}$ = 240 min pH_0 = 3.7	[14]
16 wt% Fe/SBA-15 powder	Co-condensation of Fe(III)–chloride and TEOS (470 m^2/g) ox. 550 °C	Phenol $[TOC]_0$ = 766 mg/L	X_{TOC} = 75% X_P = 100% $X_{H_2O_2}$ = *not reported*	6% (~5 mg/L)	T = 100 °C, 0.7 MPa [cat] = 0.6 g/L R = 0.75 $t_{reaction}$ = 90 min pH not controlled	[15]
30 wt% Cu/Al_2O_3 pellet (3 mm)	Molten method of Cu(II) nitrate and γ-Al_2O_3 (Alfa Aesar, 214 m^2/g) ox. 400 °C	Phenol $[TOC]_0$ = 766 mg/L	X_{TOC} = 51% X_P = 100% $X_{H_2O_2}$ = 71%	1.9% (60 mg/L)	T = 50 °C, P atm [cat] = 10.35 g/L R = 1.3 $t_{reaction}$ = 180 min pH not controlled	[8]
2.1 wt% Fe/Al_2O_3 pellet (1.1 mm)	Impregnation Fe(III) citrate on γ-Al_2O_3 (Alfa Aesar, 231 m^2/g) ox. 400 °C	Phenol $[TOC]_0$ = 3500 mg/L	X_{TOC} = 42% X_P = 100% $X_{H_2O_2}$ = 50%	60% (~11 mg/L)	T = 70 °C, P atm [cat] = 0.9 g/L R = 1.2 $t_{reaction}$ = 240 min pH not controlled	[9]
	ox. 900 °C		X_{TOC} = 36% X_P = 94% $X_{H_2O_2}$ = 40%	7% (~1 mg/L)		
0.53 wt% Fe/Al_2O_3 pellet (1.1 mm)	Impregnation Fe(III) citrate on γ-Al_2O_3 (Alfa Aesar, 231 m^2/g) ox. 900 °C	Phenol $[TOC]_0$ = 3500 mg/L	X_{TOC} = 63% X_P = 100% $X_{H_2O_2}$ = 86%	30% (~10 mg/L)	T = 70 °C, P atm [cat] = 7.2 g/L R = 0.8 $t_{reaction}$ = 240 min pH not controlled	this work

[a] The oxidant dose was reported as: $R = \frac{r_{used}}{r_{stoichiometric}}$, where $r = \frac{[mol\ H_2O_2]}{[mol\ P]}$. For instance, R = 1 represents stoichiometric H_2O_2 dosage.

Table 2
Characterization results of the support and the catalysts.

Samples	BET surface area (m^2/g)	Total iron content (wt%)
Al_2O_3	244	–
Al_2O_3-900	231	–
0.5FeAl	188	0.53
1FeAl	186	1.1
2FeAl	181	2.1
4FeAl	177	4.1

- *Scanning Electron Microscopy coupled to Energy Dispersed X-ray Spectroscopy (SEM–EDAX).* The surface morphology of the catalysts was investigated by means of a scanning electron microscope JEOL JSM-6460LV. The elemental composition of the catalysts was determined using an EDAX Genesis XM4-Sys60 equipment.
- *Raman spectroscopy.* The nature of iron species on the catalyst surface was analyzed by micro Raman spectroscopy (Renishaw inVia + Reflex spectrometer). Raman spectra were recorded at room temperature employing an Ar laser as excitation source (λ = 514 nm).
- *X-ray Photoelectron Spectroscopy (XPS).* The nature of iron species on catalyst surface was analyzed by means of a multi-technique system (SPECS) equipped with a conventional dual Mg/Al X-ray source and a Phoibos 150 analyzer operating in the fixed analyzer transmission (FAT) mode. Spectra were recorded at a pressure below 2×10^{-8} mbar. Binding energies were referred to adventitious carbon at 285 eV. The data treatment was done using the Casa XPS Processing Software.

2.2. Reaction experiments

The catalysts were tested for the oxidation of aqueous solutions of phenol using a batch reactor (250 mL) equipped with a condenser, thermocouple and a pH electrode. The experiments were performed in contact with air at atmospheric pressure and 70 °C, under vigorous stirring (1000 rpm). Since Fenton process is a heat producing reaction, the beginning of the tests was accompanied by an increase in the reactor temperature. Thus, in order to prevent the uncontrolled heating of the reaction mixture, all experiments were started at lower temperatures (between 60 and 65 °C). Once the reaction began, the temperature was maintained at the desired value by means of the temperature control of the stirring hot plate (StableTemp®, Cole-Parmer). In a typical run, the catalyst pellets were added to 100 mL of phenol aqueous solution (5 g/L). When the reaction temperature was reached, the corresponding volume of hydrogen peroxide 30 wt% (Cicarelli) was charged into the reactor and the reaction started. The final total volume was 110 mL and the resulting H_2O_2/phenol molar ratio was 11.2, which represents a sub-stoichiometric oxidant dosage according to reaction [1]:

$$C_6H_5OH + 14H_2O_2 \rightarrow 6CO_2 + 17H_2O \quad [1]$$

The experimental runs were designed changing the total iron concentration and/or the catalyst concentrations (ranges: [Fe] = 10–300 mg/L; [catalyst] = 0.9–7.2 g/L). Also, some complementary experiments were performed in the presence of different concentration of gamma-Al_2O_3 using homogeneous Fe(II) added in the form of $FeSO_4{\cdot}7H_2O$ (60–190 mg/L). Four additional commercial supports were tested: γ-Al_2O_3 (SASOL), α-Al_2O_3 (Hyflux), SiO_2 (Grace G59) and cordierite (Corning).

For all the runs, the total reaction time was 4 h. Liquid samples were taken at different time intervals and immediately analyzed. Phenol and hydrogen peroxide concentrations were measured by standard analytical techniques (colorimetric and iodometric methods, respectively) [24]; Total Organic Carbon (TOC) determinations were carried out with a Shimadzu TOC-V CPN analyzer. The pH evolution of the reaction solution was also determined.

The percentage efficiency of oxidant consumption $\eta_{H_2O_2}$ was estimated according to Eq. (1). The value of "*R*" corresponds to the ratio between the experimental oxidant to phenol molar ratio and 14 (theoretical stoichiometric). For most of the experiments the value of "*R*" was 0.8:

$$\eta_{H_2O_2}(\%) = \frac{g\ TOC_{converted}/g\ TOC_{initial}}{g\ H_2O_{2converted}/g\ H_2O_{2initial}} \cdot \frac{100}{R} \quad (1)$$

In order to confirm the repeatability of the CWHPO experiments, the reaction runs were performed at least in duplicate, obtaining a coefficient of variation Cv ⩽5% in the determinations of pH, phenol, TOC and H_2O_2 concentrations.

3. Results and discussion

3.1. Catalyst characterization

Table 2 summarizes the characterization results of the alumina and the Fe_2O_3/Al_2O_3 catalysts. Nitrogen adsorption and desorption isotherms for the fresh support and samples calcined at 900 °C (Al_2O_3 and 2FeAl) are shown in Fig. 1. All isotherms resulted in type

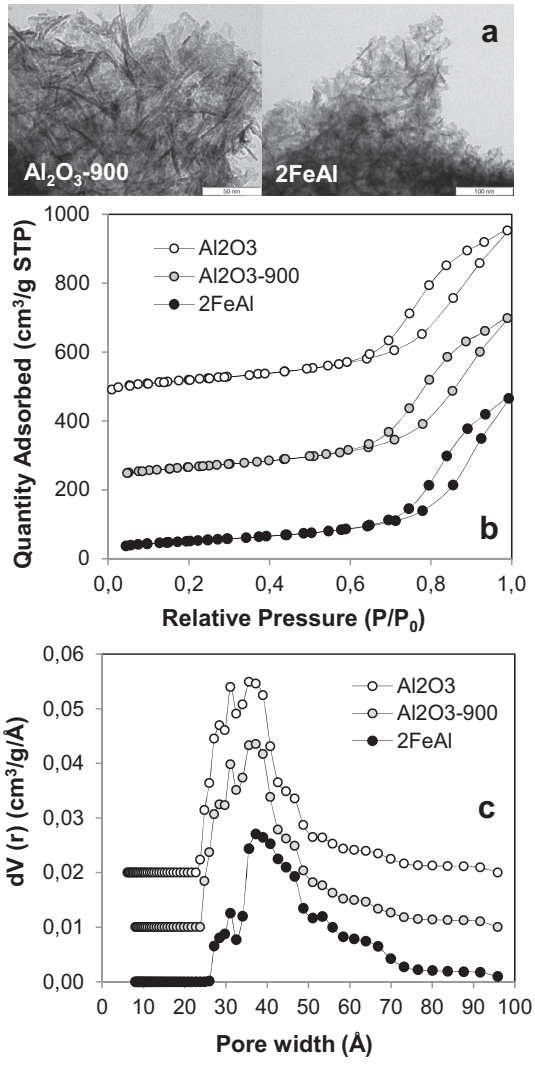

Fig. 1. TEM and N_2 physisorption results for the 2FeAl catalyst and the alumina support: (a) TEM images; (b) isotherms at −196 °C and (c) pore size distribution.

IV curves with a distinct condensation step, commonly found in mesoporous materials [25]. The hysteresis loops are apparently a combination between H1 and H3, indicating that they have slit-shape pores or plate-like particles, as confirmed by TEM images (Fig. 1a) [19]. Fresh alumina presented a specific surface area of 244 m^2/g, with a fairly narrow pore size distribution centered at around 36 Å (evaluated at the maximum of the curve) and a pore volume of 0.7 cm^3/g. The thermal treatment at 900 °C did not alter the characteristics of the support; after the calcination step the Al_2O_3-900 exhibited only a slightly decrease of the surface area, resulting in 231 m^2/g, with a pore width of 37 Å and a pore volume 0.685 cm^3/g. The incorporation of Fe species produced a decrease in the surface area and the pore volume in relation with the γ-Al_2O_3 support, suggesting that the impregnation procedure lead to a partial pore blockage by Fe particles [26]. Thus, for the 2FeAl catalyst the specific surface area and the pore volume resulted in 181 m^2/g and 0.622 cm^3/g, respectively. According to the pore size distribution and the pore volume of the catalyst, it can be observed that after Fe addition the surface characteristics of the catalyst remained similar to those of the support, suggesting good dispersion levels. In addition, due to the relatively low iron contents of the samples, the surface areas of the catalysts were practically not affected by the different iron loadings.

TEM analysis revealed a similar morphology to that previously reported by Huang et al. [19]. For certain group of gamma-alumina materials, they observed disordered plate or slit-like particles forming an open, randomly 3D stacking structure.

X-ray diffraction analysis revealed only γ-Al_2O_3 characteristic peaks; no iron phases neither mixed Fe–Al phases were detected (not shown). These observations are consistent with the conditions selected for the catalysts preparation. Both the lower iron concentrations and the impregnation method with iron citrate would have promoted the good dispersion of the Fe species onto the support that was retained even after calcination at 900 °C. According to Shaheen et al. [27], it has been demonstrated that after oxidation treatments at high temperature, alumina increases the degree of dispersion of active constituents hindering their grain growth. In terms of catalytic activity, it was observed that high Fe dispersion levels enhanced the performance of Fenton-like systems by improving H_2O_2 decomposition, and consequently hydroxyl radicals generation rate, due to a higher availability of active sites [28,29].

The surface of the different samples was analyzed by SEM–EDAX (Fig. 2). From SEM images it can be seen that catalysts with higher iron contents developed rougher surfaces. EDAX results and surface mappings confirmed a uniform distribution of iron onto the support.

The nature of Fe species was analyzed by Raman spectroscopy. The collected spectra evidenced the presence of hematite along the catalyst surface; characteristic bands of Fe_2O_3 were observed at Raman shifts of 226, 235, 292, 410, 490, 608, 649 and 1327 cm^{-1} [†]. XPS measurements also revealed that the most important iron species on catalyst surface are present as α-Fe_2O_3. Table 3 shows the binding energies of the Fe 2p3/2 main peak maximum (BE), the BE shift (eV) between samples calcined at 900 °C and the ones calcined at 400 °C and the ratio between superficial Fe (XPS) to the total Fe load (r) for 0.5FeAl and 2FeAl catalysts. From the reported BE values it can be observed that thermal treatment at 900 °C induced a shift of the Fe 2p3/2 band to higher energies in comparison with samples calcined at 400 °C with BE values ca. 710.8 eV [30]. This displacement might suggest strong interactions between Fe and support. In this sense and taking into account the size and charge of Fe^{3+}, it should not be discarded the diffusion of trivalent Fe cations into inner and/or defective zones of the Al_2O_3 network. To confirm this idea, "r" ratios were calculated; the "r" values below unity could be indicating that not all the charged iron was accessible at the catalyst surface. Moreover, in dispersed systems, neighbouring atoms are fewer than in bulk; therefore, there are fewer screening electrons and the binding energy shifts to higher values [31].

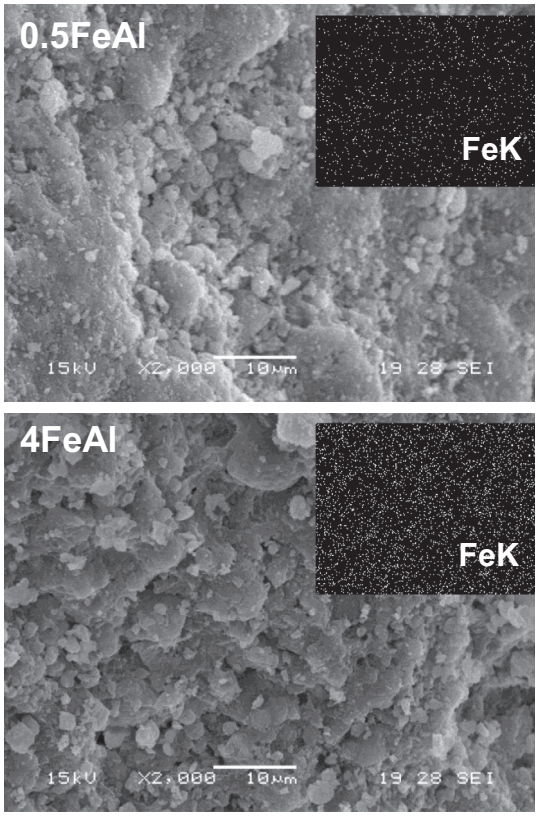

Fig. 2. SEM image (2000×) and FeK map (EDAX) of 0.5FeAl and 4FeAl catalysts.

3.2. Phenol oxidation reaction

3.2.1. Preliminary tests

Before starting CWHPO tests, several blank experiments were carried out in order to evaluate the potential contribution of non-catalytic mechanisms in phenol elimination and H_2O_2 decomposition. The thermal decomposition of phenol and hydrogen peroxide (in the absence of catalyst) were negligible at 70 °C. In the absence of H_2O_2, the phenol adsorption levels on the solids (supports and catalysts samples) remained below 6% which can be also considered as marginal.

Several experiments were also conducted without phenol. The hydrogen peroxide decomposition rates in the absence of the target organic compound were relatively high for all the catalytic systems and no induction time was observed. In a recent work, the apparent activation energy for a similar Fe_2O_3/Al_2O_3 system was estimated; the value of 52 kJ/mol [32] reasonably compares with literature reports [33,8].

3.2.2. Effect of the iron content

The catalytic runs were initially performed in the presence of a constant catalyst concentration (1.8 g/L). For this purpose, a catalyst mass of 200 mg was charged into the reactor in order to evaluate the impact of the iron content of the four different catalytic systems: 0.5FeAl; 1FeAl; 2FeAl; 4FeAl. Fig. 3 exhibits the results

[†] Espectral lines of hematite were taken from the Raman database available at Ruff.info. http://rruff.info/hematite (acceded October 24, 2014).

Table 3
XPS results of iron–alumina catalysts calcined at 400 and 900 °C.

Fresh samples	$T_{Calcination}$ (°C)	BE (eV)	"BE shift" (eV)	r
0.5FeAl	900	711.1	0.3	0.76
2FeAl	900	711.2	0.4	0.84

Note: "BE shift" was calculated as the difference between the BE of samples calcined at 900 °C and the ones calcined at 400 °C.

of phenol, TOC and H_2O_2 conversions obtained in this reactions series.

The presence of a larger number of active sites was expected to induce higher reaction rates as more hydroxyl radicals could be generated. Consequently, the iron content of the catalyst samples had a significant effect on the conversion rates and the final TOC and H_2O_2 consumption levels. As summarized in Fig. 3, the efficiency in the consumption of the oxidant increased a 20% with an eight-fold increment in the total iron (from 0.5 to 4FeAl); the TOC conversion resulted even more sensitive to the Fe content and an 87% increase of the mineralization was observed.

The application of these Fe(III) heterogeneous systems exhibited a marked induction period, as shown in Fig. 3. This observation coincides with previous works [5,9,11] using alumina-supported catalysts. We observed that the induction period was only slightly reduced with an increase of the iron content of the systems. The process of activation of the catalyst would have probably two contributions: the presence of homogeneous iron and the Fe(II)/Fe(III) ratio. Pestunova et al. [11] tested a commercial Fe_2O_3/Al_2O_3 catalyst for a second run and observed that the induction period disappeared with the repetitive use. The authors considered this as an evidence of the activation of the catalyst under reaction conditions. This activation could be associated with changes in the Fe(II)/Fe(III) ratio. Chen and Pignatello [34] investigated homogeneous systems and reported that the lag period declines as the initial concentration of ferrous ions increases. These authors indicated that the lag phase of phenol conversion was connected to the slow rate-limiting reduction of Fe^{3+} by H_2O_2 and also that the progression from the lag to the reaction phase was due to the build-up of Fe^{2+} concentration through faster reactions routes, such as the reduction of ferric species by hydroquinones and other organic species.

Supplementary experiments were carried out using 1.8 g/L of catalyst 0.5FeAl that was partially reduced. The catalyst was treated at 350 °C under hydrogen current (10 mL/min), following a similar reduction procedure as was described by Muñoz et al. [10]. The results were also included in Fig. 3. This preliminary investigation showed that in the presence of an initial amount of Fe(II) onto the catalyst, the induction period was shortened (to approximately 30 min) but it did not completely disappear. The conversion profiles for the reduced catalyst were higher than for 0.5FeAl, reaching a final mineralization of 44%. The major drawback of these reduced Fe_2O_3/Al_2O_3 systems would be their lower resistance to iron leaching, as was also reported by Muñoz et al. [10].

3.2.3. Effect of the catalyst or support concentration

Fig. 4 shows the reaction results (phenol, TOC and H_2O_2 conversions) obtained using different catalyst concentrations (range 0.9–7.2 g/L) and a constant total iron loading in the reactor ([Fe] ≈ 36 mg/L). First, different support concentrations were tested in the absence of iron and the conversion levels were practically negligible for all the experiments. In the presence of Fe species, we observed that higher catalyst concentrations gave better performances in terms of mineralization and oxidant efficiency (Fig. 4).

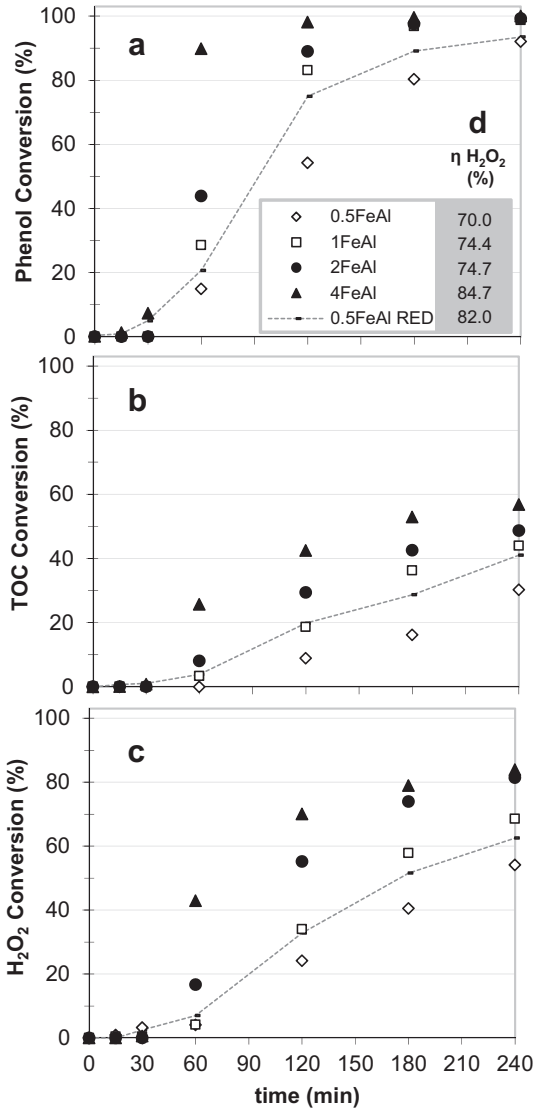

Fig. 3. Conversions as a function of reaction time, for the different Fe_2O_3/Al_2O_3 catalysts: (a) phenol conversion; (b) TOC conversion; (c) H_2O_2 conversion and (d) oxidant consumption efficiencies at final time ([cat] = 1.8 g/L; $[H_2O_2]_0$ = 0.54 M).

As confirmed by the characterization of the samples, all the catalysts exhibited a good dispersion of active species on the alumina. Nevertheless, the impact of using the same iron content dispersed on a higher amount of alumina was significant. According to the conversion profiles, the dispersion of the iron species would be enhancing the advance and the efficiency of the oxidation process. The main differences arose at higher reaction times (>120 min) for the H_2O_2 decomposition and the mineralization degrees. This might be indicating a positive effect of the dispersion of iron in the rate of hydroxyl radical generation. As the catalyst loading augmented, both the H_2O_2 and TOC conversions increased but not proportionally, resulting in an improvement of the final oxidant consumption efficiency that was close to the 92% (using 7.2 g/L of 0.5FeAl catalyst). This high percentage would evidence that the H_2O_2 decomposition routes leading to ·HO formation were strongly favoured in the system. Thus, only a minor difference between the theoretical consumption of the oxidant (estimated from mineralization results) and the measured H_2O_2 conversion was observed.

For these advanced oxidations, the hydroxyl radicals formation occurs via Fe(II) to Fe(III) reaction and most frequently, the ferric to

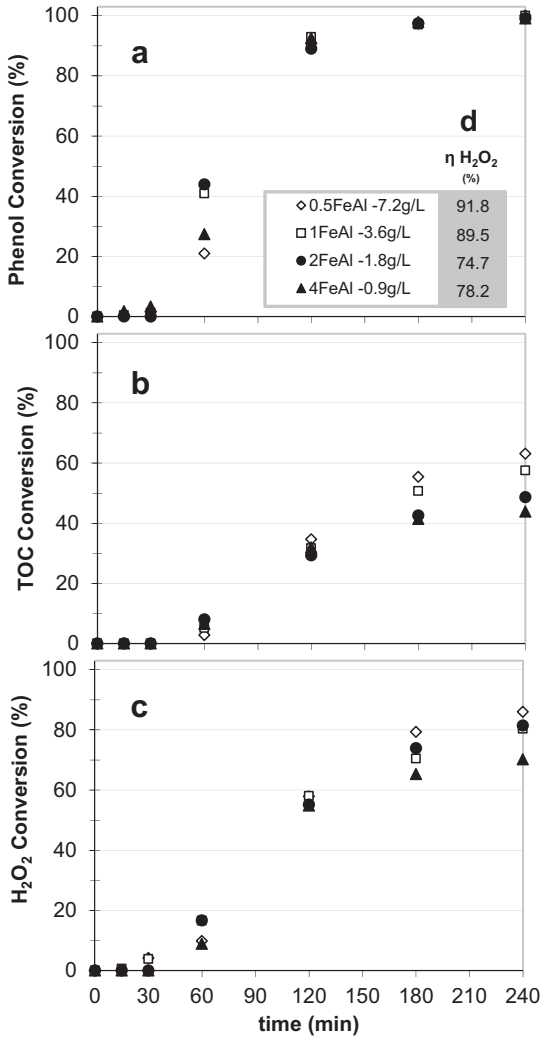

Fig. 4. Conversions as a function of reaction time at a constant Fe loading, using different catalyst concentrations: (a) phenol conversion; (b) TOC conversion; (c) H_2O_2 conversion and (d) oxidant consumption efficiencies at final time ($[Fe]_{total} \approx 36$ mg/L; $[H_2O_2]_0 = 0.54$ M).

ferrous reconversion routes are slower steps of the process. On that basis, it is likely that higher dispersion of the iron species onto the alumina could be promoting the iron redox cycle by means of Fe/Al interactions. These interactions have been previously reported for different catalytic materials [13,35]; Gabelica et al. suggested that a higher dispersion of Fe could lead to better Lewis acid–base interactions with the support, resulting in an improved performance of Fenton catalysts [13]. If so, one should expect higher H_2O_2 decomposition rates from the beginning of the reaction due to an enhanced ·HO production. However, the results of Fig. 4 do not show improvements at the initial stages of the CWHPO process for the experiments performed with higher catalyst concentrations. Rather than a direct effect on the redox cycle, the higher amount of heterogeneous catalyst might be inducing better surface interactions with the reaction intermediates formed throughout the process. Some of these organic compounds, in turn, would participate in the reduction of ferric species required for the progress of the oxidation mechanism [36,37]. Additionally, a similar kind of behaviour was recently described in a preliminary work focussed on the abatement of 1 g/L phenol solutions by Wet Air Oxidation promoted by H_2O_2 (PP-CWAO) using alumina-based catalysts. The authors observed that the adsorption of oxidation aromatic intermediates onto the alumina surface allowed the enhancement of the obtained mineralization levels in relation with experiments carried out in the absence of solid catalysts [38].

3.2.4. Catalyst stability and homogeneous contribution

The iron content of the used samples was measured. Regardless of the Fe loading or the catalyst mass used in the experiments, the leaching levels remained close to the 30%. These values are markedly below from the lixiviation percentage near 60% registered for a similar Fe_2O_3/Al_2O_3 system calcined at lower temperatures [9]. For all the experimental runs, the high initial phenol concentration led to an important accumulation of organic intermediates (some of them, carboxylic acids) and the catalysts were forced to operate at an acidic pH (2–3) during much of the CWHPO reaction time. Since these conditions strongly promote the solubilization of iron, the leaching levels that were obtained should be considered appreciable but satisfactory at this stage of the investigation, as they were in the same range than other works using analogous solid catalysts (Table 1).

The iron leaching levels cannot be neglected at the reaction conditions studied and in consequence could be contributing to the overall degradation process. For instance, in the heterogeneous experiment performed with 7.2 g/L of the 0.5FeAl catalyst, the amount of total Fe ions present in the reaction supernatant after 240 min was about 10 mg/L (ca. 30% of the total iron content). With the purpose of discriminating the potential phenol and TOC reduction due to the dissolved iron, the catalytic activity was evaluated in a phenolic solution containing 10 mg/L of Fe(II) under the same operating conditions than the heterogeneous test, giving rise to a 96% of phenol conversion and 32% of TOC removal after 240 min of reaction. Agreeing with the dynamics of hydroxyl radical generation, conversions profiles achieved almost final levels during the first 20 min of the run and then advanced slowly (as observed for the homogeneous experiments described in Section 3.2.5). However, it is noteworthy that this experiment overestimates homogeneous contribution since the release of Fe ions is a gradual process and varies with the reaction time as well as reaction conditions [8]. This fact was confirmed by the presence of an induction period at the beginning of the heterogeneous tests which indicates that the reaction is started by a heterogeneous pathway.

For a better interpretation of the role of dissolved iron species, the catalytic activity of the final supernatant with 7.2 g/L of the 0.5FeAl catalyst was assessed by adding a fresh dose of H_2O_2 ($TOC_0 = 1200$ mg/L; $[H_2O_2]_0 = 0.54$ M). After 240 min of reaction, the TOC and H_2O_2 conversions were only of 3% and 20%, respectively. This poor performance might indicate two facts, for one hand dissolved iron can be coordinated with aromatic rings or also sequestered by organic acids forming iron complexes with low catalytic activity [36,39] and/or the supernatant solution may be compounded of refractory organic intermediates which are not able of being further oxidized.

From these results it can be concluded that the heterogeneous contribution prevailed in relation with the homogeneous one.

3.2.5. Effect of catalyst support in the presence of homogeneous Fe(II)

For a more detailed study, a series of reaction runs were performed using homogeneous iron ($FeSO_4 \cdot 7H_2O$) in the presence of different amounts of gamma-alumina. These reaction results are shown in Fig. 5. The concentration of the dissolved iron was equivalent to the total iron loading used for the preceding experiments (Fig. 4).

All these reactions performed with homogeneous Fe(II) did not present induction periods. The phenol conversion profiles remained mostly unvaried for increasing alumina concentrations; however, the H_2O_2 consumption and TOC reduction increased notably, resulting in higher final mineralization levels and Etha efficiencies.

From these results, a synergistic effect due to the combination of the support and the dissolved iron species was confirmed. Alternative materials were further investigated in order to compare the impact of different porous solids as catalyst supports. The oxidation reactions were carried out using silica and cordierite ($2MgO–2Al_2O_3–5SiO_2$) in the presence of 36 mg/L of homogeneous Fe(II). The TOC conversion results are shown in Fig. 6. No improvements were observed with any of the silicate materials when compared with the homogeneous run performed in the absence of solid support. The oxidant conversion rates and phenol conversion profiles also remained unchanged. This behaviour might be related to the stronger acidity of gamma-alumina in comparison with silica–alumina and silica–magnesia materials [40].

For a better elucidation of the role of alumina, further homo/heterogeneous experiments were performed by using γ-Al_2O_3 supplied by SASOL and α-Al_2O_3 (Fig. 6). The performance of homogeneous Fe(II) in the presence of a different gamma-alumina support reached similar final conversion levels than the one provided by ALFA AESAR, giving rise to a 73% of TOC removal after 240 min of reaction. The repeatability in the conversion trends might confirm the positive influence of the surface characteristics of mesoporous aluminas and also prevents the possibility of catalytic activity due to the presence of impurity traces from the different preparation methodologies of the carriers. In contrast, by incorporating alpha-alumina to the reaction medium no enhancement in the catalytic activity was registered and final TOC conversion was only of 48%. Again, the reason for the different catalytic behaviours between γ and α phases could be directly related with significant differences in their structural and surface properties. While corundum is characterized by a low surface area and is largely used when high inertness is required, γ-Al_2O_3 is based on a defective spinel structure with cation vacancies giving place to the development of unique acidity or acido-basicity property (Lewis acid sites are compounded by unsaturated Al^{3+} ions, whereas surface basicity is provide by the presence of oxide anions). Then, the true particular sites are very likely anion–cation couples which can act synergistically [41].

So far, the variety of alternative supports that were compared is limited; however, these experiments confirmed that the effect of gamma-alumina in the Fenton process should not be generalized to other materials, even when they contain Al species in their structure (as in the case of cordierite and alpha-alumina). The positive impact of γ-Al_2O_3 should be considered in terms of its good sorption properties and Fe/Al interactions. As reported by Lim et al. [42], it can be supposed that the association with Lewis acid sites could facilitate the reduction of ferric ions by attracting the electron density from the iron center and destabilizing the Fe(III) state. In the presence of higher Al_2O_3 loadings we observed that both the TOC conversion rate and the H_2O_2 consumption increased. In the absence of catalyst support, the homogeneous reaction advanced rapidly, but then the H_2O_2 decomposition rate slowed down (after 30 min of reaction time) and so did the TOC conversion. Despite of the formation of intermediates that could intervene in the Fe(II) reconversion process, the H_2O_2 consumption rate became progressively slower in the homogeneous process probably due to partial complexation of the iron species in solution [36,37]. The presence of gamma-alumina would allow the adsorbed Fe ions to turn into ferrous species more efficiently, so that the generation of ·HO radicals is promoted and the overall oxidation may advance at a reasonable rate. As the H_2O_2 conversions were increased even at short reaction times, it could be inferred that the presence of Al_2O_3 would be promoting the hydroxyl radicals formation rate from the beginning of the reaction. Probably, the adsorbed iron species that are present in this homo/heterogeneous system resulted more active

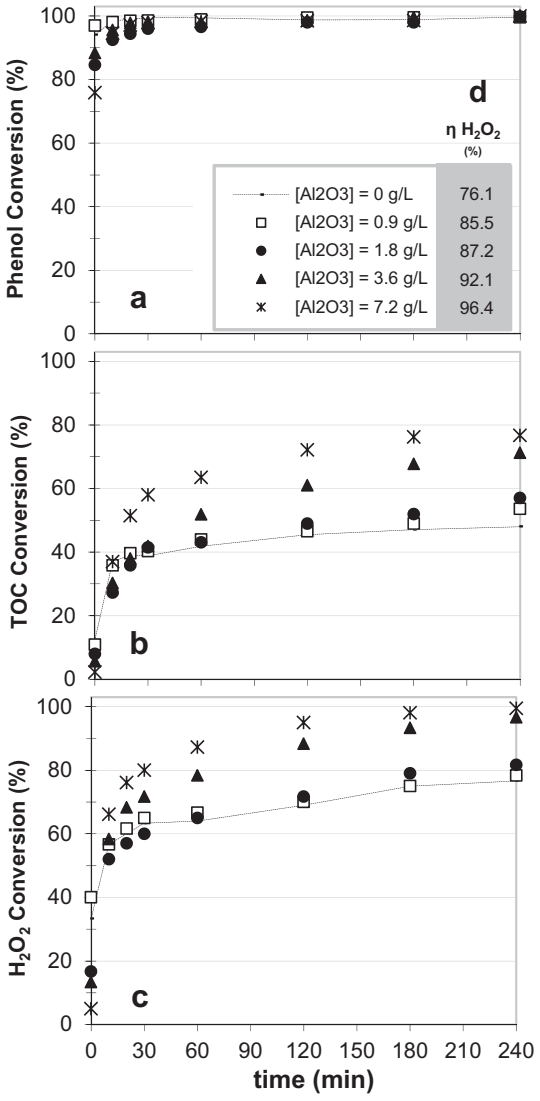

Fig. 5. Conversions as a function of reaction time, using homogeneous Fe and different Al_2O_3 loadings: (a) phenol conversion; (b) TOC conversion; (c) H_2O_2 conversion and (d) oxidant consumption efficiencies at final time ($[Fe]_{total} \approx 36$ mg/L; $[H_2O_2]_0 = 0.54$ M).

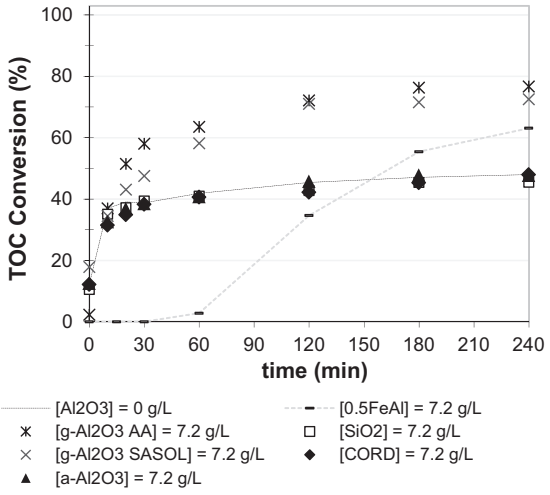

Fig. 6. TOC conversions as a function of reaction time, using different homogeneous or heterogeneous Fe systems: 0.5FeAl, homogeneous Fe(II), Fe(II) + γ-$Al_2O_{3ALFAAESAR}$, Fe(II) + γ-Al_2O_{3SASOL}, Fe(II) + α-Al_2O_3, Fe(II) + cordierite and Fe(II) + SiO_2 ($[Fe]_{total} \approx 36$ mg/L; $[H_2O_2]_0 = 0.54$ M).

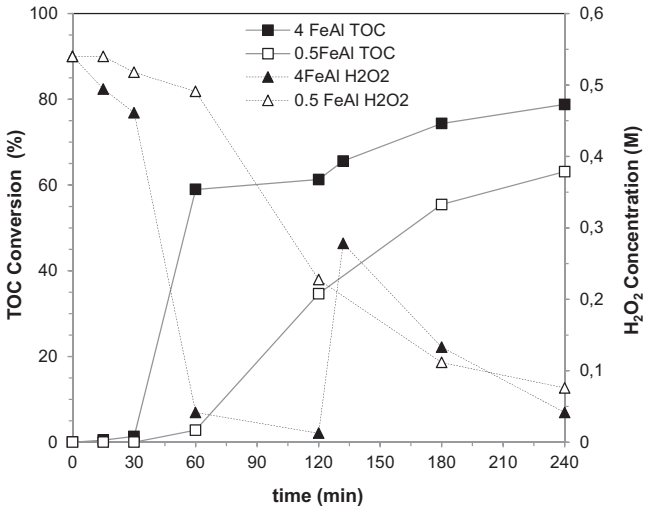

	60 min	120 min	180 min	240 min
0.5FeAl	pH=2.0	pH=2.0	pH=1.9	pH=1.9
4FeAl	pH=1.4	pH=1.9	pH=2.2	pH=2.8

Fig. 7. TOC conversion, H_2O_2 concentration and pH values as a function of reaction time, using 0.5FeAl and 4FeAl catalysts ([cat] = 7.2 g/L; $[H_2O_2]_0$ = 0.54 M).

and/or less susceptible to complexation reactions with organic species. For the experiments using 7.2 g/L of γ-Al_2O_3, the accelerated conversion of H_2O_2 to ·HO led to a practically complete consumption of the oxidant at 180 min of reaction and a high Etha efficiency of 96%.

3.2.6. Combined effect of higher iron and catalyst concentrations

As a closing, we report the experiments performed combining both higher iron content and higher catalyst loading (7.2 g/L of catalyst 4FeAl). For the sake of comparison Fig. 7 also includes the reaction results obtained using 7.2 g/L of 0.5FeAl. As indicated by the hydrogen peroxide concentration profile of 4FeAl, the oxidant was completely consumed at 120 min of reaction time and the oxidation process stopped. Then, a subsequent dose of H_2O_2 was added (27 mmol, which represents half of the initial oxidant dosage) and the reaction continued (the final mineralization levels were close to 80%). The induction time was shortened (to 30 min) and the overall CWHPO performance was notably enhanced by the increase in the initial charge of heterogeneous iron. The oxidant consumption efficiency remained near 80%. Lower accumulation of intermediate species should be inferred from these reaction parameters. This was also confirmed by the higher final pH of the solution (Fig. 7). As a consequence of these improvements, the iron leaching levels were reduced from 30% to 20%.

Additional exploratory experiments were performed using increasing doses of oxidant and higher total iron loadings and it was detected that the TOC reduction could not overcome the 80% (when 5 g/L phenol initial concentration is used). This might be an indication of the formation of refractory carboxylic intermediates (that would represent the 20% of the initial organic carbon) that were not able to be completely oxidized to CO_2 at the present conditions of the CWHPO. According to literature survey, this refractory fraction would be mainly conformed by carboxylic acids such as oxalic and acetic acids [36].

At this point, it must be considered that the treatment of concentrated phenol solutions requires the development of improved catalytic materials in order to accomplish the demands of the aggressive reaction medium. As mentioned before, the high initial phenol concentration forces the system to operate at very acidic conditions (Fig. 7, pH evolution) with important accumulation of organic intermediates.

The results using mesoporous alumina-based materials were very promising and lixiviation was reduced, but the final iron concentrations that remained in solutions were still high. Thus, further efforts are needed in order to develop more active and stable catalysts. A higher activity might be crucial to enhance catalytic stability: if the total operation period at strongly acidic pH could be shortened (by means of higher mineralization rates) and also the refractory intermediates portion could be reduced to its minimum, then the catalyst stability should be favoured. At first glance, a temperature increase would be a relatively simple way to improve the CWHPO performance [43]. However, from all the previous work accomplished in this field, there are interesting approaches that might be taken into account in order to adjust the catalyst design and the preparation procedures to carry out the oxidation processes under reaction conditions as moderate as possible. A good alternative to satisfy these requirements could be the development of ordered mesoporous alumina-based catalysts.

In general terms, the Fe/Al interactions may provide certain advantages when implementing Fenton and heterogeneous Fenton-like treatment systems.

4. Conclusions

By means of economical procedures and materials (impregnation of a γ-Al_2O_3 support using ferric citrate as iron precursor, followed by a high temperature treatment at 900 °C), mesoporous catalysts were developed, and they resulted very promissory as heterogeneous Fenton-like systems. The Fe/Al interactions promoted by the properties of the alumina support could facilitate the iron redox cycle that is implied in the progress of the organic pollutants oxidation.

Under adjusted reaction parameters, these Fe_2O_3/meso-Al_2O_3 systems exhibited an effective catalytic performance: complete phenol conversions, high mineralization levels with a maximum TOC conversion of 80% and high oxidant consumption efficiencies (between 80% and 96%). The mineralization levels achieved under soft operation conditions were high, taking into account the initial organic carbon content of the effluent, but the accumulation of refractory reaction intermediates prevented complete TOC conversions. The iron leaching resistance of the catalysts was improved; however, the effect of using a high initial phenol concentration on the catalytic stability could not be disregarded. Iron species solubilization was promoted by the presence of acidic intermediates and the resulting pH drop that was registered during the process.

A positive impact of using higher iron contents was confirmed in the range 0.003–0.11 of [Fe]/[phenol] molar ratios. An additional positive influence was noted due to the high dispersion degree of the iron species onto the alumina support. For a constant iron total loading, the iron dispersion favours the CWHPO performances, probably connected to a synergistic effect of Fe/Al interactions.

Also, for Fenton experiments (using dissolved $FeSO_4$) we observed that the presence of increasing amounts of γ-Al_2O_3 pellets in the reactor notably improved the mineralization levels (in a 64%) and the oxidant consumption efficiency (in a 27%). Alternative materials (silica, cordierite and α-Al_2O_3) were tested, showing no improvements in the homogeneous oxidation. In this regard, the favourable interaction between Fe/Al should be taken as an advantage of catalytic materials based on gamma-alumina, but also as a potential strategy to improve the classic homogeneous Fenton processes by incorporating alumina to the reaction systems configuration.

Acknowledgements

The authors gratefully acknowledge the financial support from CONICET, ANPCyT and Universidad Nacional de Mar del Plata. We

also thank Mr. H. Asencio for his technical support and Dr. J.P. Tomba for the technical assistance in Raman measurements (project PMEOG-1359).

References

[1] L.F. Liotta, M. Gruttadauria, G. Di Carlo, G. Perrini, V. Librando, J. Hazard. Mater. 162 (2009) 588–606.
[2] M. Hartmann, S. Kullmann, H. Keller, J. Mater. Chem. 20 (2010) 9002–9017.
[3] S.R. Pouran, A.A.A. Raman, W.M.A.W. Daud, J. Clean. Prod. 64 (2014) 24–35.
[4] J. Chen, Adv. Mater. Res. 955–959 (2014) 569–580.
[5] N. Al-Hayek, J.P. Eymery, M. Dore, Water Res. 19 (1985) 657–666.
[6] Y. Liu, D. Sun, J. Hazard. Mater. 143 (2006) 448–454.
[7] P. Bautista, A. Mohedano, J.A. Casas, J.A. Zazo, J.J. Rodríguez, J. Chem. Technol. Biotechnol. 86 (2011) 497–504.
[8] N.S. Inchaurrondo, P. Massa, R. Fenoglio, J. Font, P. Haure, Chem. Eng. J. 198–199 (2012) 426–434.
[9] C. di Luca, F. Ivorra, P. Massa, R. Fenoglio, Ind. Eng. Chem. Res. 51 (2012) 8979–8984.
[10] M. Muñoz, Z.M. de Pedro, N. Menendez, J.A. Casas, J.J. Rodriguez, Appl. Catal. B: Environ. 136–137 (2013) 218–224.
[11] O.P. Pestunova, O.L. Ogorodnikova, V.N. Parmon, Chem. Sust. Dev. 11 (2003) 227–232.
[12] L. Doumic, G. Salierno, M. Cassanellob, P. Haure, M. Ayude, Catal. Today 240 (2015) 67–72.
[13] Z. Gabelica, A. Charmot, R. Vataj, R. Soulimane, J. Barrault, S. Valange, J. Thermal, Anal. Calorim. 95 (2009) 445–454.
[14] J.-M. Tatibouët, E. Guélou, J. Fournier, Top. Catal. 33 (2005) 225–232.
[15] J.A. Melero, G. Calleja, F. Martínez, R. Molina, M.I. Pariente, Chem. Eng. J. 131 (2007) 245–256.
[16] Z. Zhang, R.W. Hicks, T.R. Pauly, T.J. Pinnavaia, J. Am. Chem. Soc. 124 (2002) 1592–1593.
[17] T.J. Pinnavaia, Z. Zhang, R.W. Hicks, in: A. Sayari, M. Jaroniec (Eds.), Nanoporous Materials IV (Studies in Surface Science and Catalysis, Vol. 156), Elsevier B.V., Amsterdam, 2005. pp. 1–10.
[18] A. Miyazaki, I. Balint, in: F.S. García Einschlag (Ed.), Waste Water-Treatment and Reutilization, InTech, Rijeka (Croatia), 2011. pp. 277–298.
[19] B. Huang, C.H. Bartholomew, S.J. Smith, B.F. Woodfield, Microporous Mesoporous Mater. 165 (2013) 70–78.
[20] G. Busca, S. Berardinelli, C. Resini, L. Arrighi, J. Hazard. Mater. 160 (2008) 265–288.
[21] G. Centi, S. Perathoner, T. Torre, M.G. Verduna, Catal. Today 55 (2000) 61–69.
[22] P. Gogate, A.B. Pandit, Adv. Environ. Res. 8 (2004) 501–551.
[23] S. Perathoner, G. Centi, Top. Catal. 33 (2005) 207–224.
[24] L.S. Clesceri, A. Geenberg, A. Eaton, Standard Methods for the Examination of Water and Wastewater, 12th ed., American Public Health Association, Washington, DC, 1998.
[25] K.S.W. Sing, D.H. Everett, R.A.W. Haul, L. Moscou, L.A. Pierotti, J. Rouquérol, T. Siemieniewska, Pure Appl. Chem. 57 (1985) 603–619.
[26] K.M. Parida, A.C. Pradhan, Ind. Eng. Chem. Res. 49 (2010) 8310–8318.
[27] W. Shaheen, K. Hong, Thermochim. Acta 381 (2002) 153–164.
[28] J.H. Ramirez, F.J. Maldonado-Hódar, A.F. Pérez-Cadenas, C. Moreno-Castilla, C.A. Costa, L.M. Madeira, Appl. Catal. B: Environ. 75 (2007) 312–323.
[29] L.C.A. Oliveira, M. Gonçalves, M.C. Guerreiro, T.C. Ramalho, J.D. Fabris, M.C. Pereira, K. Sapag, Appl. Catal. A: Gen. 316 (2007) 117–124.
[30] T.L. Barr, J. Phys. Chem. 12 (1978) 1801–1810.
[31] Z. Kónia, J. Kiss, A. Oszkó, A. Siska, I. Kiricsi, Phys. Chem. Chem. Phys. 3 (2001) 155–158.
[32] C. di Luca, F. Ivorra, P. Massa, R. Fenoglio, F. Medina Cabello, Curr. Catal. 3 (2014) 161–165.
[33] S. Lin, M.D. Gurol, Environ. Sci. Technol. 32 (1998) 1417–1423.
[34] R. Chen, J.J. Pignatello, Environ. Sci. Technol. 31 (1997) 2399–2406.
[35] A. Balu, A. Pineda, K. Yoshida, J.M. Campelo, P.L. Gai, R. Luque, A.A. Romero, Chem. Commun. 46 (2010) 7825–7827.
[36] J.A. Zazo, J.A. Casas, A.F. Mohedano, M.A. Gilarranz, J.J. Rodriguez, Environ. Sci. Technol. 39 (2005) 9295–9302.
[37] R.F.F. Pontes, J.E.F. Moraes, A. Machulek Jr., J.M. Pinto, J. Hazard. Mater. 176 (2010) 402–413.
[38] S. García-Figueruelo, M. Muñoz, Z.M. de Pedro, A. Quintanilla, J.A. Casas, J.J. Rodriguez, in: S. Esplugas (Ed.), Chemical Engineering for Sustainable Development, Proc. 13MCC, Barcelona, Spain, SEQUI, Barcelona, 2014, p. 228.
[39] F. Mijangos, F. Varona, N. Villota, Environ. Sci. Technol. 40 (2006) 5538–5543.
[40] D.S. Maciver, H.H. Tobin, R.T. Barth, J. Catal. 2 (1963) 485–497.
[41] G. Busca, Catal. Today 226 (2014) 2–13.
[42] H. Lim, J. Lee, S. Jin, J. Kim, J. Yoon, T. Hyeon, Chem. Commun. 4 (2006) 463–465.
[43] J.A. Zazo, G. Pliego, S. Blasco, J.A. Casas, J.J. Rodriguez, Ind. Eng. Chem. Res. 50 (2011) 866–870.